frontiers | Frontiers in Earth Science

ORIGINAL RESEARCH
published: 06 July 2022
doi: 10.3389/feart.2022.888443

Extended-Range Luminescence Dating of Central and Eastern Amazonia Sandy Terrains

Fernanda Costa G. Rodrigues[1], Naomi Porat[2], Thays Desiree Mineli[1], Ian Del Río[1], Pontien Niyonzima[1], Luciana Nogueira[1], Fabiano do Nascimento Pupim[1,3], Cleverson Guizan Silva[4], Paul Baker[5], Sherilyn Fritz[6], Ingo Wahnfried[7], Gustavo Kiefer[8] and André Oliveira Sawakuchi[1]*

[1]Luminescence and Gamma Spectrometry Laboratory (LEGaL), Institute of Geosciences, University of São Paulo, São Paulo, Brazil, [2]Geological Survey of Israel, Jerusalem, Israel, [3]Department of Environmental Sciences, Federal University of São Paulo, São Paulo, Brazil, [4]Institute of Geosciences, Fluminense Federal University, Niterói, Brazil, [5]Division of Earth and Ocean Sciences, Duke University, Durham, NC, United States, [6]Department of Earth and Atmospheric Sciences, University of Nebraska, Lincoln, Durham, NC, United States, [7]Geosciences Department, Amazonas Federal University, Manaus, Brazil, [8]Brazil Potash, Manaus, Brazil

OPEN ACCESS

Edited by:
David K. Wright, University of Oslo, Norway

Reviewed by:
Luigi Jovane, University of São Paulo, Brazil
Manoj Kumar Jaiswal, Indian Institute of Science Education and Research Kolkata, India
Andrew Murray, Aarhus University, Denmark

***Correspondence:**
Fernanda Costa G. Rodrigues
cgrfernanda@usp.br
cgr.fernanda@gmail.com

Specialty section:
This article was submitted to Quaternary Science, Geomorphology and Paleoenvironment, a section of the journal Frontiers in Earth Science

Received: *02 March 2022*
Accepted: *13 June 2022*
Published: *06 July 2022*

Citation:
Rodrigues FCG, Porat N, Mineli TD, Del Río I, Niyonzima P, Nogueira L, Pupim FdN, Silva CG, Baker P, Fritz S, Wahnfried I, Kiefer G and Sawakuchi AO (2022) Extended-Range Luminescence Dating of Central and Eastern Amazonia Sandy Terrains. Front. Earth Sci. 10:888443. doi: 10.3389/feart.2022.888443

The Amazonia biome hosts upland closed and open vegetation ecosystems, in which the current biogeographical patterns relate to the evolution of the physical landscape. Therefore, understanding the origin and timing of the substrates supporting different ecosystems is indispensable for better comprehension of Amazonian biogeography. Here we used quartz optically stimulated luminescence (OSL) and thermally transferred optically stimulated luminescence (TT-OSL) for dating sandy substrates of closed and open vegetation environments in Central and Eastern Amazonia, from both outcrop and drill core samples (Autazes core: PBAT-15-43). These sandy substrates present ages ranging from 1 ka up to almost 2 Ma, that were primarily interpreted as depositional ages of fluvial terraces. Moreover, ages are discussed in terms of potential geomorphic processes leading to the formation of substrates, such as soil mixing and apparent age of quartz from the parent bedrock. The coupling between OSL and TT-OSL techniques allow us to date sedimentary deposits covering the whole Quaternary, which implies a new time window for the Amazonia history.

Keywords: TT-OSL dating, Amazonia sandy terrains, fluvial deposits, landscape evolution, geochronology

INTRODUCTION

The evolution of Amazonian biota and its remarkable biodiversity are intricately linked to the evolution of the physical landscape, and the formation of the transcontinental drainage system is proposed as a main driver for biotic diversification within the Amazonian biome (Hoorn et al., 2010; Ribas et al., 2012; Boubli et al., 2015). In addition to the well-known closed upland rainforest, Amazonia also hosts isolated patches of open vegetation, such as savannas and white-sand ecosystems (WSE) (Anderson, 1981; Adeney et al., 2016), which are considered important environments that drove biodiversification in upland Amazonia (Haffer, 1969) and other ancestral regions (Frasier et al., 2008). Therefore, extended-range chronologies of sedimentary substrates supporting upland vegetation in Amazonia are crucial to understand the evolution of the landscape during the Quaternary and Neogene and its relation to the current biodiversity and biogeographical patterns of the biome. The Pliocene and Quaternary lowland fluvial record in Central Amazonia is composed of heavily weathered siliciclastic and non-fossiliferous

deposits, suitable for the application of quartz-based dating techniques (e.g., Soares et al., 2010; Pupim et al., 2019; Bezerra et al., 2022), as feldspar is frequently lacking due to heavy weathering. Most of the reliable ages that constrain sedimentation in these sequences are based on optically stimulated luminescence (OSL) dating of quartz (e.g., Rossetti et al., 2015; Cremon et al., 2016; Pupim et al., 2019) and are restricted to the last 300 ka.

OSL is the light arising from charges trapped in crystal lattice defects when quartz is exposed to ionizing radiation and subsequently released and recombined when quartz is exposed to stimulation light. Measuring the natural OSL signal allows the determination of radiation dose absorbed by quartz during burial, and sediment depositional ages are estimated by dividing the radiation dose (Gy) by the environmental dose rate (Gy/ka). Several extended-range luminescence dating methods were proposed with the potential to date as far as the Early Pleistocene, including thermally transferred optically stimulated luminescence (TT-OSL), with reported equivalent dose (D_e) values up to 2,500 Gy (Wang et al., 2006a). The TT-OSL signal is measured by depleting the OSL signal, applying a heat treatment ≥260°C to transfer charges from TT-OSL traps into OSL traps, and remeasuring the OSL signal (Wang et al., 2006a; Adamiec et al., 2010). The charge transfer has been hypothesized as a double transfer, where electrons from OSL traps are released and stored in a refuge trap, before being thermally transferred back (Wang et al., 2006a) or alternatively as a single transfer, where electrons are thermally transferred from a source trap to an OSL trap (Adamiec et al., 2010). The TT-OSL signal is represented as 1) the recuperated OSL (Re-OSL), which makes up about 90% of the signal and is more sensitive to light, and 2) the basic-transferred OSL (BT-OSL) (Aitken, 1998; Duller and Wintle, 2012), which makes up the remaining 10%. Both multiple-aliquot (MAR) and single-aliquot (SAR) regenerative dose protocols have been proposed to estimate D_e using the TT-OSL signal (e.g., Wang et al., 2006a; Porat et al., 2009; Adamiec et al., 2010; Chapot et al., 2016).

Despite the routine use of TT-OSL dating in recent years, only few studies use this technique in geological settings of South America (e.g., Pupim et al., 2016; Bezerra et al., 2022). In addition to the understating of the evolution of the Amazonian landscape in the Pliocene and Quaternary, TT-OSL dating protocols still need to be tested in different geological contexts, including South America, as quartz OSL properties are not uniform and also vary at a grain-to-grain level (Preusser et al., 2009), and the same might be valid for the TT-OSL signal. In this study, we used both quartz OSL and TT-OSL for dating upland sandy deposits covered by open and closed vegetation in lowland Central and Eastern Amazonia. The formation chronology of these deposits allows us to understand how upland terrains bounding the Amazon River floodplains were assembled in periods beyond the late Pleistocene.

STUDY SITES AND SAMPLING

This study used two datasets from Central Amazonia and two from Eastern Amazonia (**Figure 1** and **Table 1**). The Eastern Amazonia dataset comprises outcrop samples from sandy substrates of savannas exposed in pits and road cuttings, for which the depositional and/or weathering origin is still under debate. Eastern Amazonia sandy substrates are composed of massive, loose, medium, and poorly to moderately sorted light reddish to brownish sands (AVA01—**Figures 2A,B**). The Central Amazonia datasets comprise both outcrop samples from substrates of open vegetation ecosystems (i.e., WSE), composed of massive, loose, and coarse white sands (AVA22—**Figures 2C,D**), and drill core samples composed of heavily weathered fluvial sandstones and siltstones (Autazes Core: PBAT-15-43, **Figures 2E,F**). These sand substrates cover Pliocene-Miocene and late Cretaceous-Paleogene fluvial deposits from the Novo Remanso and Alter do Chão Formations (Gautheron et al., 2022).

Outcrop samples were collected in aluminum or opaque PVC tubes to avoid sunlight exposure. Drill core samples were wrapped in aluminum foil, and only the inner sections were used for luminescence analysis while the outer section exposed to light was used for determination of radionuclides concentrations needed for dose rate estimation. Sediments within a radius of 30 cm from the luminescence sampling point in the outcrops were collected separately to estimate radiation dose rates.

SAMPLE PREPARATION AND MEASUREMENTS

Sample preparation and measurements were carried out under subdued orange-red light. The preparation procedures of quartz concentrates included wet sieving to separate the 180–250 μm fraction; dissolving organic matter with 35% H_2O_2 and carbonates with 10% HCl solutions; density separation at 2.75 g/cm^3 and 2.62 g/cm^3 with lithium metatungstate (LMT) solution to isolate quartz grains from heavy minerals and feldspar grains; and etching in concentrated 40% HF solution for 40 min to eliminate the outer rind of quartz grains affected by alpha radiation and remnant feldspar grains. Density separation showed that little to no feldspar was present in the studied samples.

All measurements were performed using two Risø DA-20 TL/OSL readers and a Lexsyg Smart reader, all equipped with ^{90}Sr/^{90}Y beta source (dose rates of 0.07, 0.12 and 0.11 Gy/s respectively), blue and infrared LEDs for stimulation, and a 7.5 mm Hoya U-340 filter for light detection in the ultraviolet band. Aliquots of 4–9 mm diameter were prepared using adhesive silicone spray on stainless steel discs or cups. OSL-IRSL depletion ratio was used to confirm that there was no feldspar contamination in the quartz aliquots (Duller, 2003).

The SAR protocols used to determine the D_e using the OSL (Murray and Wintle, 2000) and TT-OSL (Porat et al., 2009) signals are described in **Table 2**. The OSL SAR protocol was also used to estimate the characteristic dose (D_0) of dose response curves, and $2D_0$ was considered to appraise the upper limit for OSL dating in the studied sediment samples (Wintle and Murray, 2006). The intervals used to derive both OSL and TT-OSL signals were the integral of the first 1 s of light emission, minus the last

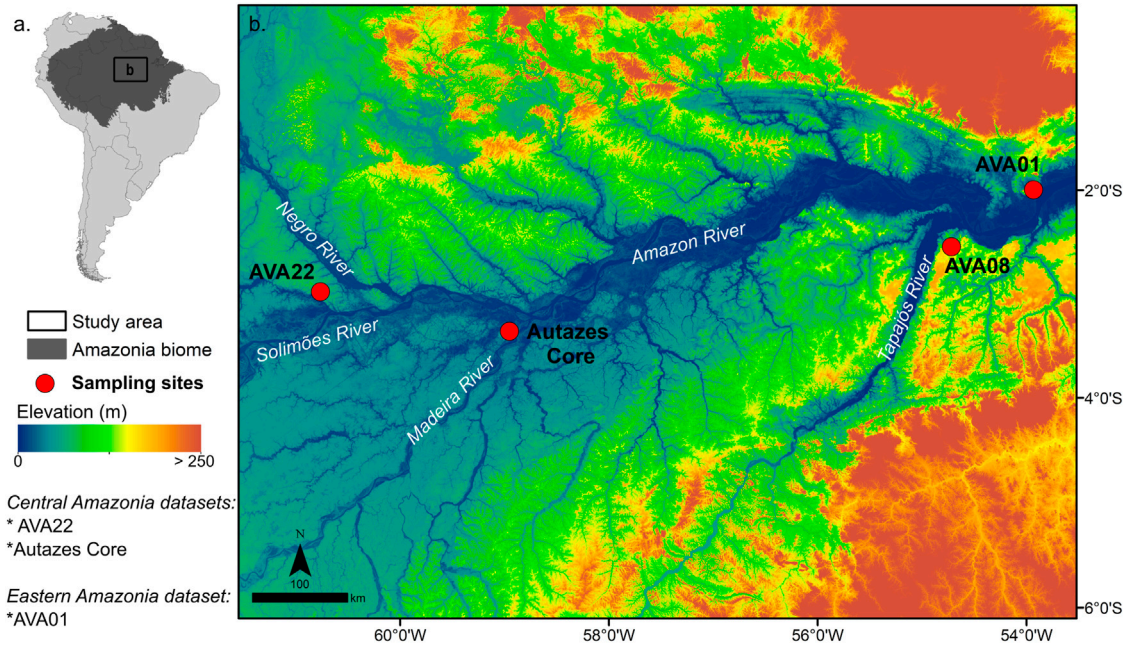

FIGURE 1 | (A) Location of the Amazonia biome within South America and study area within this biome; **(B)** digital elevation model (DEM; from Shuttle Radar Topography Mission—SRTM) and sampling locations in Central (AVA22 and Autazes core) and Eastern (AVA01 and AVA08) lowland Amazonia.

10 s as background. Dose-response curves (DRC) were fitted using a linear, single saturating exponential, or an exponential plus linear functions. D_e was calculated using the unweighted arithmetic mean (empirical average) of individual dose estimates, as suggested by (Guérin et al., 2017), accepting recycling ratios between 0.9–1.1 and 0.8–1.2 and recuperation up to 5% and 10%, for OSL and TT-OSL, respectively. The suitability of both OSL and TT-OSL SAR protocols for estimation of D_e under laboratory conditions was evaluated by dose recovery tests (data summary of dose recovery tests on **Supplementary Tables S1, S2**). The dose recovery tests performed by Bezerra et al. (2022) on samples from the same study area were also used for evaluation of the suitability of the TT-OSL protocol. OSL average calculated-to-given dose ratio is 0.96, and TT-OSL average calculated-to-given dose ratio is 1.5 (**Supplementary Table S2**).

D1 < D2 < D3 < D4, D5 = 0 Gy, D6 = D1, D7 =D1 (with infrared stimulation before blue led stimulation).

The concentrations of U, Th, and K for determination of dose rates were measured using high-resolution gamma spectrometry with a high-purity germanium detector (Canberra Instruments, relative efficiency of 55% and energy resolution of 2.1 keV at 1,332 keV) encased in an ultralow background shield. Inductively coupled plasma mass spectrometry (ICP-MS) was also used for determination of U and Th concentrations and inductively coupled plasma atomic emission spectroscopy (ICP-OES) was used to determine K concentration. U, Th, and K concentration uncertainties from gamma spectrometry are 1σ. ICP-MS U and Th uncertainties are 5 % and 10%, respectively. ICP-OES K uncertainty is 3%. The concentrations of U (ppm), Th (ppm), and K (%) were converted into dose rates (Gy/ka) using the conversion factors proposed by Guérin et al. (2011). Cosmic rays' contribution to the dose rate was calculated according to Prescott and Hutton (1994), considering the latitude, longitude, altitude, current depth below the surface, and density of each sample. The internal dose rate was assumed as 0.01 Gy/ka, as this value is considered the upper limit to the internal alpha dose rate in quartz (Vandenberghe et al., 2008).

RESULTS

Representative OSL and TT-OSL decay curves and DRC of Eastern and Central Amazonia study sites are shown in **Figure 3**. All samples have the OSL curve dominated by the fast component in the first 1 s, with the OSL signal decaying slightly slower in Central Amazonia samples. The TT-OSL signal also decays slower in Central Amazonia samples. All samples have saturated natural OSL signals, except for the two shallowest samples of the Autazes Core, at 0.2 and 1.8 m depth, which have D_e of 4.6 ± 0.5 Gy and 94.6 ± 4.7 Gy, respectively (**Table 3**), and for sample AVA08, with D_e of 52.3 ± 3.5 Gy. The OSL $2D_0$ of all samples ranges from 90 to 180 Gy (**Table 3**), indicating the limits of OSL dating. TT-OSL D_e ranges from 92 ± 9 Gy to 1,692 ± 229 Gy in Central Amazonia samples and from 161 ± 10 Gy to 747 ± 74 Gy in Eastern Amazonia samples (**Table 3** and **Figure 5A**). Overdispersion of the TT-OSL D_e distribution varies from 16% to 61% (**Table 3** and exemplary D_e distribution on **Figures 4B,D,F**). All samples have high sensitivity changes meaning that the test dose signal increases with SAR cycles as a response to the same beta dose, with more

FIGURE 2 | (A) AVA01 outcrop in Eastern Amazonia with savanna sandy substrate covering late Cretaceous-Paleogene sandstones from the Alter do Chão Formation (dashed black line indicates the upper boundary of the Alter do Chão sandstones); **(B)** close-up image of the savanna sandy substrate in AVA01; **(C)** AVA22 outcrop of sandy deposits covered by white-sand vegetation (*campina*) in Central Amazonia; **(D)** close up image of the sandy substrate of white-sand vegetation; **(E)** Autazes drill core weathered sandstones and siltstones from 0 to 10.42 m depth (from left to right), **(F)** Autazes drill core weathered sandstones and siltstones from 10.42 to 18.85 m depth (from left to right).

TABLE 1 | Summary information of samples used in this study.

	Sampling	Sample code	Lab code	Latitude	Longitude	Depth (m)
Eastern Amazonia	Outcrop	AVA01C	L1083	−2.009195°	−54.094106°	0.5
		AVA01E	L1084	−2.009195°	−54.094106°	1.0
		AVA01G	L1085	−2.009195°	−54.094106°	1.5
		AVA08B	L1106	−2.553336°	−54.960837°	1.0
Central Amazonia	Outcrop	AVA22A	L1436	−3.115015°	−60.746138°	0.8
		AVA22C	L1438	−3.115015°	−60.746138°	1.4
		AVA22E	L1440	−3.115015°	−60.746138°	2.0
	Autazes core (PBAT-15–43)	155812	L1490	−3.494253°	−58.973555°	0.2
		155813	L1491	−3.494253°	−58.973555°	1.8
		155814	L1492	−3.494253°	−58.973555°	2.7
		155815	L1493	−3.494253°	−58.973555°	4.9
		155816	L1488	−3.494253°	−58.973555°	5.8
		155817	L1487	−3.494253°	−58.973555°	6.6
		155818	L1486	−3.494253°	−58.973555°	11.4
		155819	L1485	−3.494253°	−58.973555°	13.7

TABLE 2 | Single-aliquot regenerative-dose (SAR) OSL and TT-OSL protocols used to estimate equivalent doses (D_e) from quartz aliquots in this study.

Step	OSL (Murray and Wintle, 2000)	TT-OSL (Porat et al. 2009)
1	Give dose Di (natural signal, i = 0 and D0 = natural dose)	Give dose Di (natural signal, i = 0 and D0 = natural dose)
2	Preheat at 240°C for 10 s	Preheat at 260°C for 10 s
3	OSL at 125°C for 40 s (Li)	OSL at 125°C for 200 s
4	Give a test dose of 10 or 25 Gy	Preheat at 260°C for 10 s
5	Preheat at 160°C for 10 s	TT-OSL: OSL at 125°C for 100 s (Li)
6	OSL at 125°C for 40 s (Ti)	Give a test dose of 10 or 50 Gy
7	Blue LED illumination at 280°C for 40 s	Preheat at 200 or 240°C for 10 s
8	—	OSL at 125°C for 100 s (Ti)
9	—	Deplete remaining TT-OSL: OSL at 350°C for 100 s

D1 < D2 < D3 < D4, D5 = 0 Gy, D6 = D1, D7 =D1 (with infrared stimulation before blue led stimulation)

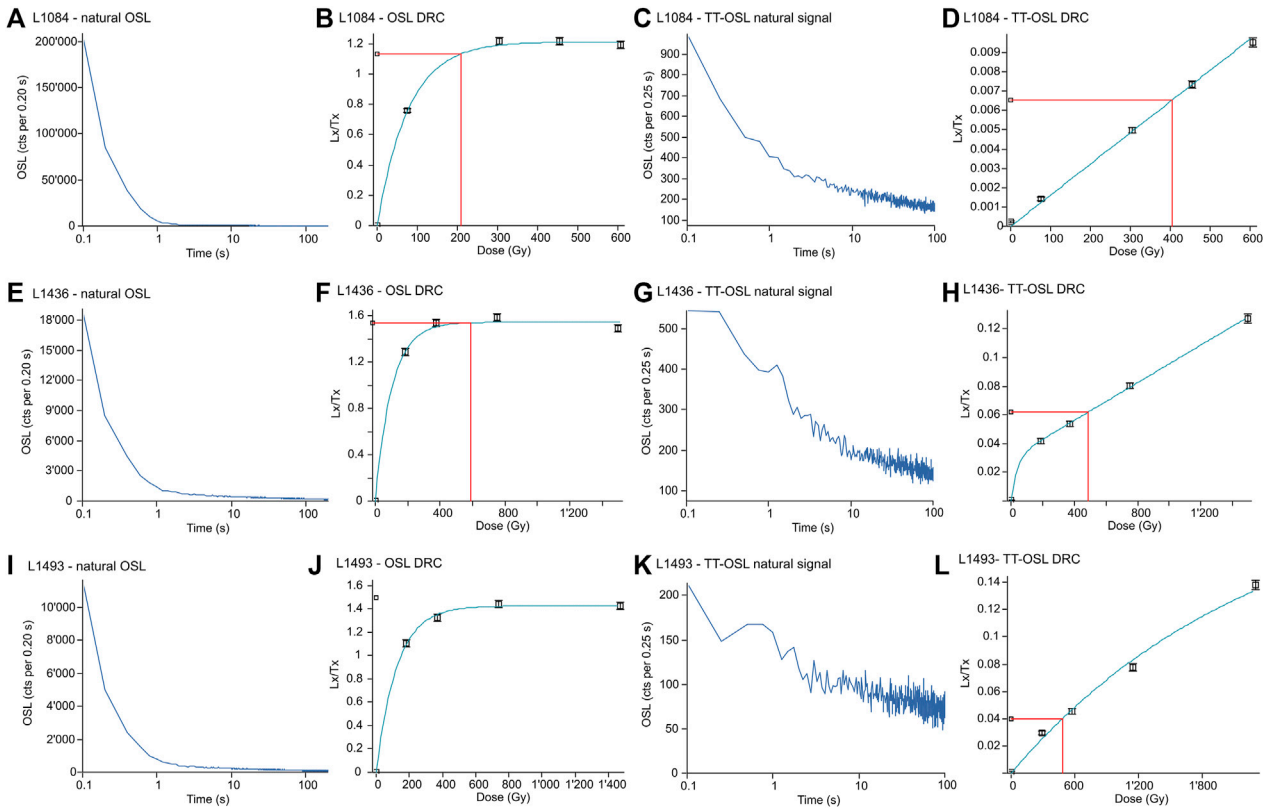

FIGURE 3 | Natural OSL **(A,E,I)** and TT-OSL **(C,G,K)** signals of representative samples of the study sites and their respective DRCs **(B,F,J)** for OSL and **(D,H,L)** for TT-OSL. Sample L1084 - outcrop in eastern Amazonia; sample L1436 - outcrop in central Amazonia; sample L1493 - Autazes core in central Amazonia.

significant increases occurring on the AVA22 samples (**Figures 4A,C,E**). The difference between TT-OSL D_e and OSL D_e for samples AVA08B, 155812, and 155813 is 109 Gy, 87 Gy, and 142 Gy, respectively.

The Autazes core has a trend of increasing D_e with depth, and the Eastern and Central Amazonia outcrop depth profiles (AVA01 and AVA22) present statistically indistinguishable values. Dose rates are lower in the outcrops in Central and Eastern Amazonia (~0.6 Gy/ka) than in the Autazes core (~3.6 Gy/ka) (**Figure 5A**). All samples have less than 1% of K content, and U is usually higher in Central Amazonia samples (both AVA22 and Autazes core) than in Eastern Amazonia (**Figures 5B–D**; **Supplementary Material S1**). The Th content in the Autazes core is ~20x higher than in the outcrop profiles (AVA01 and AVA22) (**Figure 5D** and **Supplementary Material S1**). Ages in the Eastern Amazonia AVA01 profile range from 1927 ± 246 ka to 1,239 ± 294 ka and ages in the Central Amazonia AVA22 profile range from 1,058 ± 198 ka to 923 ± 142 ka (**Table 3**; **Figure 6**). In the Autazes core, the TT-OSL ages obtained are younger than the ages from other outcrop

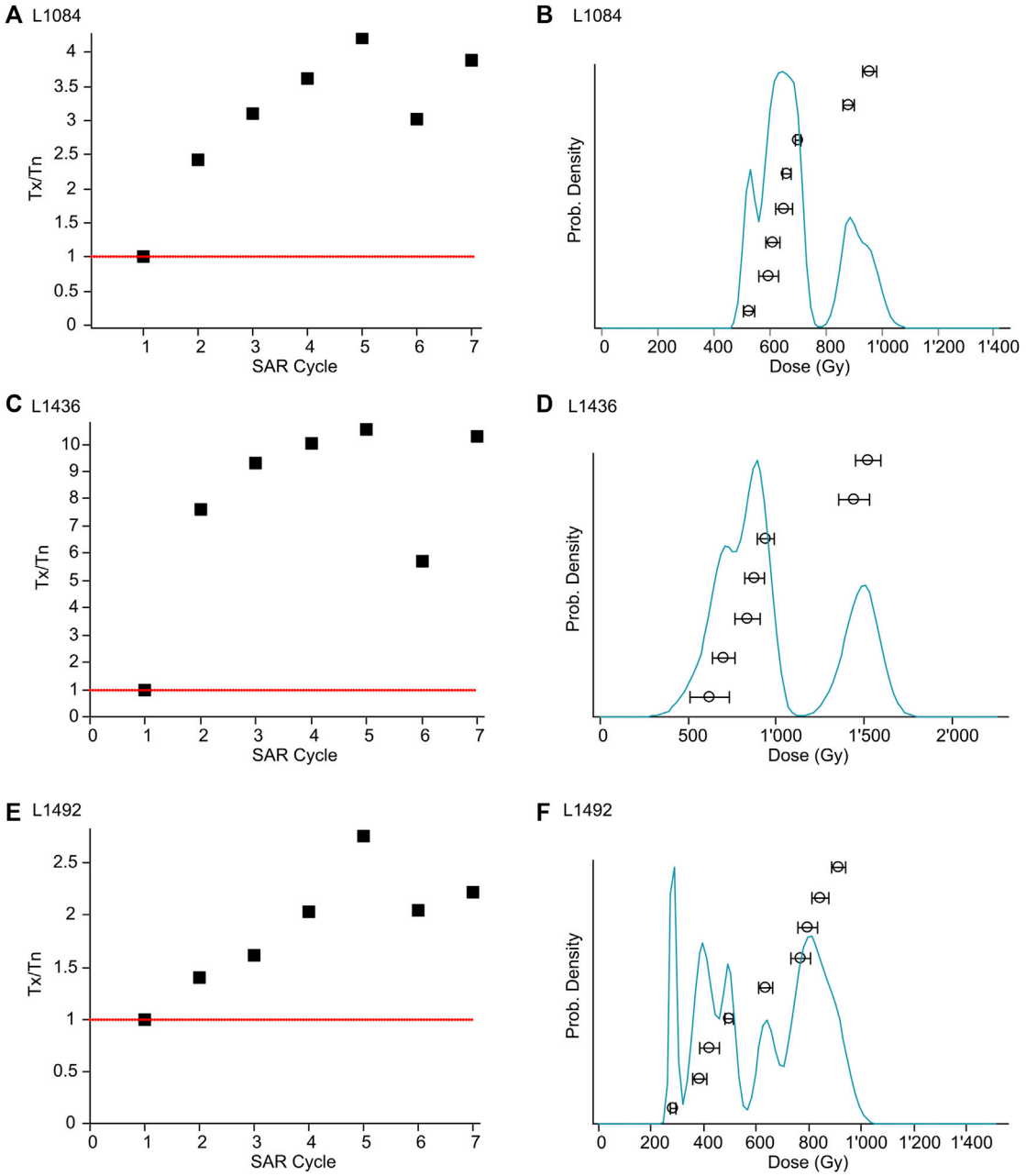

FIGURE 4 | Sensitivity changes over each SAR cycle and TT-OSL De distributions of representative samples AVA01E (L1084 - **A,B**), AVA22A (L1436 - **C,D**), and 155814 (L1492 - **E,F**).

profiles, ranging from 585 ± 85 ka to 23 ± 3 ka (**Table 3**; **Figure 6**).

DISCUSSION

TT-OSL Equivalent Doses and Burial Ages

TT-OSL ages obtained here can be interpreted as: 1) the sand deposition age; 2) *in situ* weathering over older sedimentary fluvial deposits that give rise to soils, with the D_e representing the time since the last solar exposure due to soil mixing (Gray et al., 2020); or 3) the minimum age of the parent rock, because of the thermal instability or saturation of TT-OSL signals (Faershtein et al., 2018). Hence, the TT-OSL ages calculated for the different sandy substrates may be interpreted as ages of sediment deposition, soil mixing processes, or an apparent age of quartz from the parent bedrock.

TABLE 3 | Summary of OSL and TT-OSL dating results.

Location	Sample	Lab Code	N	D_e (Gy)	OD (%)	Dose rate (Gy/ka)	Age (ka)	OSL $2D_0$
Eastern Amazonia (outcrop)	AVA01C	L1083	7	562 ± 90	36	0.46 ± 0.08	1239 ± 294	120
	AVA01E	L1084	7	713 ± 57	19	0.41 ± 0.04	1789 ± 237	130
	AVA01G	L1085	8	747 ± 74	23	0.40 ± 0.03	1927 ± 246	105
	AVA08B*	L1106	23	52.3 ± 3.5	23	0.93 ± 0.07	56.6 ± 5.7	—
	AVA08B	L1106	2	161 ± 10	—	0.93 ± 0.07	174 ± 17	—
Central Amazonia (outcrop)	AVA22A	L1436	7	992 ± 133	29	1.08 ± 0.08	923 ± 142	152
	AVA22C	L1438	9	997 ± 92	32	0.86 ± 0.06	1167 ± 137	170
	AVA22E	L1440	4	1595 ± 275	27	1.52 ± 0.11	1058 ± 198	139
Central Amazonia (Autazes core)	155812*	L1490	19	4.6 ± 0.5	44	3.96 ± 0.36	1.2 ± 0.2	—
	155813*	L1491	12	94.6 ± 4.7	16	3.86 ± 0.36	24.6 ± 2.6	112
	155812	L1490	7	92.0 ± 8.8	21	3.96 ± 0.36	23.3 ± 3.1	—
	155813	L1491	6	237 ± 27	26	3.86 ± 0.36	61.6 ± 9.1	112
	155814	L1492	9	612 ± 76	38	3.99 ± 0.37	153 ± 24	180
	155815	L1493	7	504 ± 162	61	3.69 ± 0.35	137 ± 46	141
	155816	L1488	7	848 ± 76	24	2.53 ± 0.26	336 ± 46	130
	155817	L1487	12	834 ± 125	51	3.46 ± 0.33	242 ± 83	129
	155818	L1486	7	1096 ± 186	42	4.01 ± 0.38	274 ± 53	148

**OSL results.*

OD is the overdispersion of D_e distributions and N is the number of aliquots per sample.

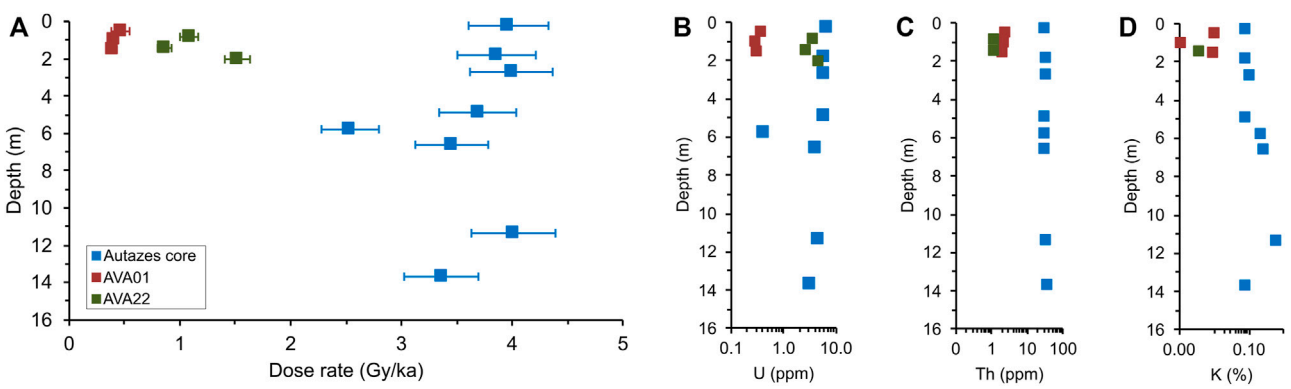

FIGURE 5 | (A) Dose rate, **(B)** U concentration, **(C)** Th concentration and **(D)** K concentration versus depth in sediment profiles of the sutdy area.

One of the main concerns when using the TT-OSL signal for sediment dating is its relatively low thermal stability (Li and Li, 2006; Chapot et al., 2016; Faershtein et al., 2018). A luminescence trap is considered thermally stable for periods lower than τ/10 (where τ is the trap lifetime) (Aitken, 1998). The quartz OSL fast component, which is used for luminescence dating in the late Pleistocene and Holocene age range, has a trap lifetime of around 300 Ma at 10°C (Jain et al., 2003; Singarayer and Bailey, 2003). Thus, it is considered stable in a million years (Ma) timespan and the maximum age limit is imposed by quartz OSL signal saturation. On the other hand, the TT-OSL main trap has a lifetime of 4–7 Ma at 10–20°C (Adamiec et al., 2010; Shen et al., 2011; Thiel et al., 2012; Faershtein et al., 2018) or even lower, of 180–760 ka at 10–20°C (Li and Li, 2006; Chapot et al., 2016), which would imply age limit in the hundred thousand years timespan due to thermal instability. Hence, thermal loss affects the TT-OSL signal in the Ma-scale age range, and even ages in the range of only a few hundred thousand years may be underestimated (Adamiec et al., 2010; Shen et al., 2011; Chapot et al., 2016; Faershtein et al., 2018). Another point for caution is the considerably slower rate of optical resetting of the TT-OSL signal compared with the fast OSL component. It might take weeks of natural sunlight exposure to deplete TT-OSL signals (e.g., Jacobs et al., 2011; Arnold et al., 2013; Demuro et al., 2015). These concerns should be addressed carefully. However, TT-OSL ages agree with independent age control in many cases (e.g., Pickering et al., 2013; Arnold et al., 2015; Hernandez et al., 2015), suggesting that quartz from different geological settings has an heterogenous behavior regarding TT-OSL thermal loss and bleaching suitability.

The calculated-to-given dose ratio of ~1.5 for the TT-OSL signal points to significant overestimation of D_e, possibly

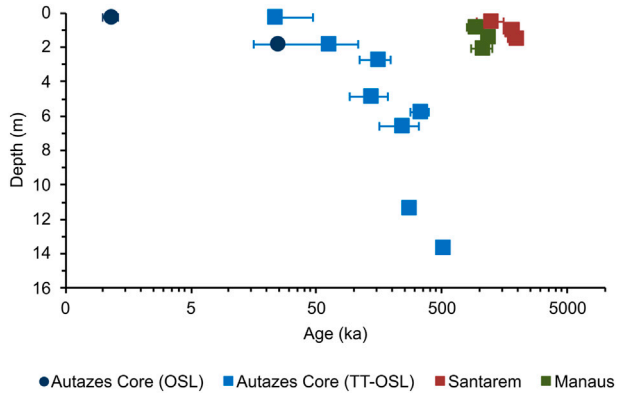

FIGURE 6 | OSL and TT-OSL ages versus depth for the studied samples.

related to incomplete bleaching of the signal. This is also shown by the difference between OSL and TT-OSL D_e in the same samples, that ranges from 87 to 142 Gy, implying an overestimation of ~20–40 ka for Central Amazonia and of ~117 ka for Eastern Amazonia. TT-OSL signals bleach slower than the OSL signal, and they are not reduced to zero (Tsukamoto et al., 2008), having residual doses ranging from 5 to 40 Gy, depending on the depositional environment (Wang et al., 2006a; Tsukamoto et al., 2008; Jacobs et al., 2011; Duller and Wintle, 2012; Demuro et al., 2015). In the case of D_e relative to sedimentation ages, this implies that fluvial processes in lowland Amazonia are not enough for completely resetting the TT-OSL signal. If on one hand, there is overestimation of 20–117 ka due to residual doses, there might be an unaccounted for underestimation of the D_e due to the TT-OSL thermal instability.

Independent age control for the studied sediment samples from Central Amazonia is given by (U-Th)/He ages on supergene lateritic duricrusts and iron-enriched horizons within the Miocene-Pliocene fluvial sandstones (Gautheron et al., 2022) representing the substrate of the studied sandy deposits. (U-Th)/He ages indicate that such sandstones were deposited and weathered in the last ~3 to 1 Ma (Gautheron et al., 2022). Therefore, the maximum depositional age of studied sandy substrates from Central Amazonia is from the late Pliocene and Pleistocene. This chronostratigraphic framework agrees with the interpretation of our TT-OSL ages as representing the timing of sediment deposition. Although the possibility of the TT-OSL ages indicating only the minimum age cannot be ruled out, considering the low thermal stability of TT-OSL signals (Li and Li, 2006; Chapot et al., 2016; Faershtein et al., 2018). Our TT-OSL ages ranging from almost 2 Ma matches other fluvial terraces of the Amazon River with TT-OSL depositional ages ranging from 556 to 1,063 ka (Bezerra et al., 2022). The much younger OSL ages at the top of the Autazes core, from 1 to 25 ka, might represent the accumulation of fluvial sediments during major flooding events during the Late Pleistocene and Holocene (Pupim et al., 2019).

Geomorphic Implications

OSL and TT-OSL ages constrain the formation of open and closed vegetation sandy substrates in lowland Amazonia, in both shallower and deeper profiles, extending the dated ages based on luminescence dating methods. The terraces dated previously using TT-OSL (Pupim et al., 2016; Bezerra et al., 2022) and the Autazes drill core (Kiefer et al., 2019) have both surface features and sedimentary structures that suggest fluvial deposition. However, many sandy terrains covered by savanna-like vegetation in lowland Amazonia lack surface depositional features or sedimentary structures, and correspond to massive, weathered sands covering Cretaceous-Paleogene and Miocene-Pliocene fluvial sandstones (Gautheron et al., 2022). The massive sandy constitution observed in the Eastern Amazonia and Central Amazonia open-vegetation sampling sites hinders the identification of a depositional or pedogenetic origin. The interpretation of TT-OSL ages as sediment deposition ages suggests fluvial systems with a higher base level and wider ancient floodplains across lowland Central and Eastern Amazonia during the Mid and Early Pleistocene. Fluvial sediments with Mid Pleistocene TT-OSL ages also were observed in terraces along the lower Xingu River (Pupim et al., 2016), eastward the study areas.

In Central Amazonia, after the deposition of these sandy terrains and their colonization by vegetation, their transformation into "white-sands" occurred due to podzolization processes in the last ~1.2 Ma (sample AVA22C). Podzolization occurs by repeated rising and falling of the water table, which leaches organic matter and clays from the upper soil horizon, creating the light-colored sandy E horizon, and deposits them lower in the soil profile as the B horizon (Lundström et al., 2000). The main correlate for the white-sand ecosystems is the hydromorphic spodosols, occurring in the middle and upper Negro River basin (Adeney et al., 2016) and interpreted as *in situ* weathering of ancient deposits, like the Late Cretaceous sandstones of the Alter do Chão Formation (Horbe et al., 2004). Age constraints for deposition of substrates of these white-sand ecosystems are needed to appraise if spodosols developed over ancient sandstones, such as the Late Cretaceous Alter do Chão Formation, or over Pleistocene sediments covering older rocky substrates. The first view implies the long-lasting occurrence of white-sand substrates beyond the Pleistocene while the second points to Pleistocene landscape shift driven by fluvial incision events followed by weathering of abandoned sandy deposits in uplands.

CONCLUSION

Quartz grains representative of lowland Amazonia sandy substrates colonized by open and closed vegetation ecosystems were used for SAR OSL and TT-OSL dating. The ages obtained in study sites of Central and Eastern Amazonia can represent the time of: 1) sediment deposition, 2) soil mixing processes, or 3) the minimum age of the weathered parent rock. Comparison between TT-OSL ages and (U-Th)/He ages from underlying iron crusts

suggests that the sandy substrates can be formed by weathering of fluvial sediments accumulated during the Pleistocene, despite other interpretations cannot be ruled out. In Eastern Amazonia savanna sandy substrate, TT-OSL ages ranged from 1927 to 1,239 ka. The Autazes core in Central Amazonia comprises heavily weathered fluvial sandstones and siltstones, covered by upland closed rainforest, with OSL ages from ~25 to 1 ka in the upper 2 m of the record. The OSL signal is saturated in downcore samples, where TT-OSL ages range from 505 to 23 ka until 14 m depth. TT-OSL ages obtained for the sandy substrate of WSE in Central Amazonia are in the 1,167-923 ka range. The difference between OSL and TT-OSL ages for the same samples suggests that TT-OSL ages have an overestimation of ~20 to 117 ka. Assuming that the TT-OSL ages represent sediment deposition ages, we can interpret fluvial systems with a higher base level and wider floodplains in Central and Eastern Amazonia during the mid-Pleistocene. In this case, savanna and WSE in the study areas expanded over fluvial deposits during the Pleistocene.

DATA AVAILABILITY STATEMENT

The original contributions presented in the study are included in the article/**Supplementary Material**, further inquiries can be directed to the corresponding author.

AUTHOR CONTRIBUTIONS

FR, NP, and AS contributed to conception and design of the study and wrote the first draft of the manuscript. FR carried out experiments and data analysis with the help of NP, TM, IR, LN, and PN. FP contributed with applications of extended-range luminescence dating techniques in Amazonian fluvial deposits. GK was responsible for the drilling and logging of the Autazes core. CGS and PB got access to the Autazes core through an agreement between the Fluminense Federal University (UFF) and Potash Brazil. AS, CS, PB, SF, and IW raised funding and defined sampling intervals and sampled the Autazes core. All authors contributed to manuscript revision, read, and approved the submitted version.

FUNDING

This research had the financial support of the Trans-Amazon Drilling Project (ICDP, US-NSF grants #EAR-1812857 and #EAR-1812681, FAPESP grant #2018/23899-2 and STRI), São Palo Research Foundation (FAPESP grants #16/02656-9; #18/15123-4) and Conselho Nacional de Desenvolvimento Científico e Tecnológico (CNPq grant #062.01355/2018). FR, IR, and PN are supported by the FAPESP (grants #18/12472-8, #19/20588-9, #19/04059-6). AS and FP are supported by CNPq (grants #304727/2017-2; #302411/2018-6). Luminescence analyses were made in a laboratory created under the auspices of FAPESP (grant #09/53988-8).

ACKNOWLEDGMENTS

We thank João P. S. de Cortes, Thomas K. Akabane, and Julio I. B. Silva for their fieldwork assistance. We also thank Brazil Potash for providing the Autazes core samples and sampling support. We also thank the Amazonian Biodiversity Studies Centre for the permission for fieldwork. We would like to thank the reviewers for taking the time and effort, and for the valuable comments and suggestions, which helped us to improve the quality of our manuscript.

SUPPLEMENTARY MATERIAL

The Supplementary Material for this article can be found online at: https://www.frontiersin.org/articles/10.3389/feart.2022.888443/full#supplementary-material

REFERENCES

Adamiec, G., Duller, G. A. T., Roberts, H. M., and Wintle, A. G. (2010). Improving the TT-OSL SAR Protocol through Source Trap Characterisation. *Radiat. Meas.* 45, 768–777. doi:10.1016/j.radmeas.2010.03.009

Adeney, J. M., Christensen, N. L., Vicentini, A., and Cohn-Haft, M. (2016). White-sand Ecosystems in Amazonia. *Biotropica* 48, 7–23. doi:10.1111/btp.12293

Aitken, M. J. (1998). *Introduction to Optical Dating: The Dating of Quaternary Sediments by the Use of Photon-Stimulated Luminescence*. New York: Claredon Press.

Anderson, A. B. (1981). White-sand Vegetation of Brazilian Amazonia. *Biotropica* 13, 199–210. doi:10.2307/2388125

Arnold, L. J., Demuro, M., Navazo, M., Benito-Calvo, A., and Pérez-González, A. (2013). OSL dating of the Middle Palaeolithic Hotel California site, Sierra de Atapuerca, north-central Spain. *Boreas* 42, 285–305. doi:10.1111/j.1502-3885.2012.00262.x

Arnold, L. J., Demuro, M., Parés, J. M., Pérez-González, A., Arsuaga, J. L., Bermúdez de Castro, J. M., et al. (2015). Evaluating the Suitability of Extended-Range Luminescence Dating Techniques over Early and Middle Pleistocene Timescales: Published Datasets and Case Studies from Atapuerca, Spain. *Quat. Int.* 389, 167–190. doi:10.1016/j.quaint.2014.08.010

Bezerra, I. S. A. A., Nogueira, A. C. R., Motta, M. B., Sawakuchi, A. O., Mineli, T. D., Silva, A. d. Q., et al. (2022). Incision and Aggradation Phases of the Amazon River in Central-Eastern Amazonia during the Late Neogene and Quaternary. *Geomorphology* 399, 108073. doi:10.1016/j.geomorph.2021.108073

Boubli, J. P., Ribas, C., Lynch Alfaro, J. W., Alfaro, M. E., da Silva, M. N. F., Pinho, G. M., et al. (2015). Spatial and Temporal Patterns of Diversification on the Amazon: A Test of the Riverine Hypothesis for All Diurnal Primates of Rio Negro and Rio Branco in Brazil. *Mol. Phylogenetics Evol.* 82, 400–412. doi:10.1016/j.ympev.2014.09.005

Chapot, M. S., Roberts, H. M., Duller, G. A. T., and Lai, Z. P. (2016). Natural and Laboratory TT-OSL Dose Response Curves: Testing the Lifetime of the TT-OSL Signal in Nature. *Radiat. Meas.* 85, 41–50. doi:10.1016/j.radmeas.2015.11.008

Cremon, É. H., Rossetti, D. d. F., Sawakuchi, A. d. O., and Cohen, M. C. L. (2016). The Role of Tectonics and Climate in the Late Quaternary Evolution of a

Northern Amazonian River. *Geomorphology* 271, 22–39. doi:10.1016/j.geomorph.2016.07.030

Demuro, M., Arnold, L. J., Parés, J. M., and Sala, R. (2015). Extended-range Luminescence Chronologies Suggest Potentially Complex Bone Accumulation Histories at the Early-To-Middle Pleistocene Palaeontological Site of Huéscar-1 (Guadix-Baza Basin, Spain). *Quat. Int.* 389, 191–212. doi:10.1016/j.quaint.2014.08.035

Duller, G. A. T. (2003). Distinguishing Quartz and Feldspar in Single Grain Luminescence Measurements. *Radiat. Meas.* 37, 161–165. doi:10.1016/S1350-4487(02)00170-1

Duller, G. A. T., and Wintle, A. G. (2012). A Review of the Thermally Transferred Optically Stimulated Luminescence Signal from Quartz for Dating Sediments. *Quat. Geochronol.* 7, 6–20. doi:10.1016/j.quageo.2011.09.003

Faershtein, G., Guralnik, B., Lambert, R., Matmon, A., and Porat, N. (2018). Investigating the Thermal Stability of TT-OSL Main Source Trap. *Radiat. Meas.* 119, 102–111. doi:10.1016/j.radmeas.2018.09.010

Frasier, C., Albert, V. A., and Struwe, L. (2008). Amazonian Lowland, White Sand Areas as Ancestral Regions for South American Biodiversity: Biogeographic and Phylogenetic Patterns in Potalia (Angiospermae: Gentianaceae). *Org. Divers. Evol.* 8, 44–57. doi:10.1016/j.ode.2006.11.003

Gautheron, C., Sawakuchi, A. O., dos Santos Albuquerque, M. F., Cabriolu, C., Parra, M., Ribas, C. C., et al. (2022). Cenozoic Weathering of Fluvial Terraces and Emergence of Biogeographic Boundaries in Central Amazonia. *Glob. Planet. Change* 212, 103815. doi:10.1016/j.gloplacha.2022.103815

Gray, H. J., Keen-Zebert, A., Furbish, D. J., Tucker, G. E., and Mahan, S. A. (2020). Depth-dependent Soil Mixing Persists across Climate Zones. *Proc. Natl. Acad. Sci. U.S.A.* 117, 8750–8756. doi:10.1073/pnas.1914140117

Guérin, G., Christophe, C., Philippe, A., Murray, A. S., Thomsen, K. J., Tribolo, C., et al. (2017). Absorbed Dose, Equivalent Dose, Measured Dose Rates, and Implications for OSL Age Estimates: Introducing the Average Dose Model. *Quat. Geochronol.* 41, 163–173. doi:10.1016/j.quageo.2017.04.002

Guérin, G., Mercier, N., and Adamiec, G. (2011). Dose-rate Conversion Factors: Update. *Anc. TL* 29, 5–8.

Haffer, J. (1969). Speciation in Amazonian Forest Birds. *Science* 165, 131–137. doi:10.1126/science.165.3889.131

Hernandez, M., Bahain, J.-J., Mercier, N., Tombret, O., Falguères, C., and Jaubert, J. (2015). Dating Results on Sedimentary Quartz, Bones and Teeth from the Middle Pleistocene Archaeological Site of Coudoulous I (Lot, SW France): A Comparative Study between TT-OSL and ESR/U-series Methods. *Quat. Geochronol.* 30, 493–497. doi:10.1016/j.quageo.2015.06.003

Hoorn, C., Wesselingh, F. P., ter Steege, H., Bermudez, M. A., Mora, A., Sevink, J., et al. (2010). Amazonia through Time: Andean Uplift, Climate Change, Landscape Evolution, and Biodiversity. *Science* 330, 927–931. doi:10.1126/science.1194585

Horbe, A. M. C., Horbe, M. A., and Suguio, K. (2004). Tropical Spodosols in Northeastern Amazonas State, Brazil. *Geoderma* 119, 55–68. doi:10.1016/S0016-7061(03)00233-7

Jacobs, Z., Roberts, R. G., Lachlan, T. J., Karkanas, P., Marean, C. W., and Roberts, D. L. (2011). Development of the SAR TT-OSL Procedure for Dating Middle Pleistocene Dune and Shallow Marine Deposits along the Southern Cape Coast of South Africa. *Quat. Geochronol.* 6, 491–513. doi:10.1016/j.quageo.2011.04.003

Jain, M., Murray, A. S., and Bøtter-Jensen, L. (2003). Characterisation of Blue-Light Stimulated Luminescence Components in Different Quartz Samples: Implications for Dose Measurement. *Radiat. Meas.* 37, 441–449. doi:10.1016/S1350-4487(03)00052-0

Kiefer, G. L. S., Uhlein, A., and Fanton, J. J. (2019). O Depósito Potassífero De Autazes No Contexto Estratigráfico Da Bacia Do Amazonas. *Geociencias* 38, 349–365. doi:10.5016/geociencias.v38i2.12857

Li, B., and Li, S.-H. (2006). Studies of Thermal Stability of Charges Associated with Thermal Transfer of OSL from Quartz. *J. Phys. D. Appl. Phys.* 39, 2941–2949. doi:10.1088/0022-3727/39/14/011

Lundström, U. S., Van Breemen, N., and Bain, D. (2000). The Podzolization Process. A Review. *Geoderma* 94, 91–107. doi:10.1016/S0016-7061(99)00036-1

Murray, A. S., and Wintle, A. G. (2000). Luminescence Dating of Quartz Using an Improved Single-Aliquot Regenerative-Dose Protocol. *Radiat. Meas.* 32, 57–73. doi:10.1016/S1350-4487(99)00253-X

Pickering, R., Jacobs, Z., Herries, A. I. R., Karkanas, P., Bar-Matthews, M., Woodhead, J. D., et al. (2013). Paleoanthropologically Significant South African Sea Caves Dated to 1.1-1.0 Million Years Using a Combination of U-Pb, TT-OSL and Palaeomagnetism. *Quat. Sci. Rev.* 65, 39–52. doi:10.1016/j.quascirev.2012.12.016

Porat, N., Duller, G. A. T., Roberts, H. M., and Wintle, A. G. (2009). A Simplified SAR Protocol for TT-OSL. *Radiat. Meas.* 44, 538–542. doi:10.1016/j.radmeas.2008.12.004

Prescott, J. R., and Hutton, J. T. (1994). Cosmic Ray Contributions to Dose Rates for Luminescence and ESR Dating: Large Depths and Long-Term Time Variations. *Radiat. Meas.* 23, 497–500. doi:10.1016/1350-4487(94)90086-8

Preusser, F., Chithambo, M. L., Götte, T., Martini, M., Ramseyer, K., Sendezera, E. J., et al. (2009). Quartz as a Natural Luminescence Dosimeter. *Earth-Science Rev.* 97, 184–214. doi:10.1016/j.earscirev.2009.09.006

Pupim, F. d. N., Sawakuchi, A. O., Mineli, T. D., and Nogueira, L. (2016). Evaluating Isothermal Thermoluminescence and Thermally Transferred Optically Stimulated Luminescence for Dating of Pleistocene Sediments in Amazonia. *Quat. Geochronol.* 36, 28–37. doi:10.1016/j.quageo.2016.08.003

Pupim, F. N., Sawakuchi, A. O., Almeida, R. P., Ribas, C. C., Kern, A. K., Hartmann, G. A., et al. (2019). Chronology of Terra Firme Formation in Amazonian Lowlands Reveals a Dynamic Quaternary Landscape. *Quat. Sci. Rev.* 210, 154–163. doi:10.1016/j.quascirev.2019.03.008

Ribas, C. C., Aleixo, A., Nogueira, A. C. R., Miyaki, C. Y., and Cracraft, J. (2012). A Palaeobiogeographic Model for Biotic Diversification within Amazonia over the Past Three Million Years. *Proc. R. Soc. B* 279, 681–689. doi:10.1098/rspb.2011.1120

Rossetti, D. F., Cohen, M. C. L., Tatumi, S. H., Sawakuchi, A. O., Cremon, É. H., Mittani, J. C. R., et al. (2015). Mid-Late Pleistocene OSL Chronology in Western Amazonia and Implications for the Transcontinental Amazon Pathway. *Sediment. Geol.* 330, 1–15. doi:10.1016/j.sedgeo.2015.10.001

Shen, Z. X., Mauz, B., and Lang, A. (2011). Source-trap Characterization of Thermally Transferred OSL in Quartz. *J. Phys. D. Appl. Phys.* 44, 295405. doi:10.1088/0022-3727/44/29/295405

Singarayer, J. S., and Bailey, R. M. (2003). Further Investigations of the Quartz Optically Stimulated Luminescence Components Using Linear Modulation. *Radiat. Meas.* 37, 451–458. doi:10.1016/S1350-4487(03)00062-3

Soares, E. A. A., Tatumi, S. H., and Riccomini, C. (2010). OSL Age Determinations of Pleistocene Fluvial Deposits in Central Amazonia. *An. Acad. Bras. Ciênc.* 82, 691–699. doi:10.1590/S0001-37652010000300017

Thiel, C., Buylaert, J.-P., Murray, A. S., Elmejdoub, N., and Jedoui, Y. (2012). A Comparison of TT-OSL and Post-IR IRSL Dating of Coastal Deposits on Cap Bon Peninsula, North-Eastern Tunisia. *Quat. Geochronol.* 10, 209–217. doi:10.1016/j.quageo.2012.03.010

Tsukamoto, S., Duller, G. A. T., and Wintle, A. G. (2008). Characteristics of Thermally Transferred Optically Stimulated Luminescence (TT-OSL) in Quartz and its Potential for Dating Sediments. *Radiat. Meas.* 43, 1204–1218. doi:10.1016/j.radmeas.2008.02.018

Vandenberghe, D., De Corte, F., Buylaert, J.-P., Kučera, J., and Van den haute, P. (2008). On the Internal Radioactivity in Quartz. *Radiat. Meas.* 43, 771–775. doi:10.1016/j.radmeas.2008.01.016

Wang, X. L., Lu, Y. C., and Wintle, A. G. (2006a). Recuperated OSL Dating of Fine-Grained Quartz in Chinese Loess. *Quat. Geochronol.* 1, 89–100. doi:10.1016/j.quageo.2006.05.020

Wang, X. L., Wintle, A. G., and Lu, Y. C. (2006b). Thermally Transferred Luminescence in Fine-Grained Quartz from Chinese Loess: Basic Observations. *Radiat. Meas.* 41, 649–658. doi:10.1016/j.radmeas.2006.01.001

Wintle, A. G., and Murray, A. S. (2006). A Review of Quartz Optically Stimulated Luminescence Characteristics and Their Relevance in Single-Aliquot Regeneration Dating Protocols. *Radiat. Meas.* 41, 369–391. doi:10.1016/j.radmeas.2005.11.001

Conflict of Interest: The authors declare that the research was conducted in the absence of any commercial or financial relationships that could be construed as a potential conflict of interest.

Publisher's Note: All claims expressed in this article are solely those of the authors and do not necessarily represent those of their affiliated organizations, or those of the publisher, the editors and the reviewers. Any product that may be evaluated in this article, or claim that may be made by its manufacturer, is not guaranteed or endorsed by the publisher.